Tetrahedron 69 (2013) 6317–6322

Contents lists available at SciVerse ScienceDirect

Tetrahedron

journal homepage: www.elsevier.com/locate/tet

Diarylfluorenes-based π-stacked molecules: synthesis, X-ray crystallography, and supramolecular light-emitting devices

Yang Yang [a], Jian-Feng Zhao [a], Ran-Ran Liu [a], Jie-Wei Li [a], Ming-Dong Yi [a], Guo-Hua Xie [c], Ling-Hai Xie [a,*], Yong-Zheng Chang [a], Cheng-Rong Yin [a], Xin-Hui Zhou [a], Yi Zhao [c], Yan Qian [a], Wei Huang [a,b,*]

[a] *Center for Molecular Systems and Organic Devices (CMSOD), Key Laboratory for Organic Electronics & Information Displays (KLOEID) and Institute of Advanced Materials (IAM), Nanjing University of Posts & Telecommunications (NUPT), Nanjing 210046, China*

[b] *Jiangsu-Singapore Joint Research Center for Organic/Bio-Electronics & Information Displays and Institute of Advanced Materials, Nanjing University of Technology, Nanjing 211816, China*

[c] *State Key Laboratory on Integrated Optoelectronics, College of Electronics Science and Engineering, Jilin University, 2699 Qianjin Street, Changchun 130012, China*

ARTICLE INFO

Article history:
Received 31 August 2012
Received in revised form 17 February 2013
Accepted 26 February 2013
Available online 15 March 2013

Keywords:
π-Stacks
Diarylfluorenes
Friedel–Crafts reaction
Organic complex
Non-covalent bond

ABSTRACT

A series of intramolecular π-stacked molecules as new-concept supramolecular organic semiconductors have been designed by means of the *ortho*-substituted steric hindrance of diarylfluorenes and facile synthesized via the key step of $BF_3 \cdot Et_2O$-mediated Friedel–Crafts reaction of carbinols. Their intramolecular π–π stacking interactions were corroborated by the X-ray crystallography, NMR, as well as theoretical simulation. The supramolecular organic light-emitting devices exhibited an anomalous electroluminescence with a maximum luminance of ca. 1282 cd/m^2, a luminous efficiency of 0.24 cd/A, and a turn-on voltage of 9 V. The π-stacked semiconductors are potential models of supramolecular semiconductors and optoelectronics.

1. Introduction

Supramolecular interactions in biomolecules and materials have been attracted much attention after the concept of supramolecular chemistry proposed by Lehn,[1] and many effects have been made to explore the intermolecular supramolecular systems.[2] For example, they have been designed for the detector of explosive TNT,[3] molecular tweezers as well as other molecular machines.[4] In contrast, intramolecular supramolecular molecules have been neglected in the past two decades in despite of the discovery of DNA with the intramolecular π-stacked motifs.[5] In fact, intramolecular π-stacked motifs have exhibited unique conformational change for nonvolatile flash memories and other unique properties in the area of organic electronics.[6] Besides, intramolecular π-stacked systems have also been used as fluorescence-based sensors,[7] probe[8] and offer an effective channel for triplet energy transfer and excimer emissions.[8,9] Up to date, several scaffolds, including norbornane,[10] 1,8-diarylbiphenylene,[11] naphthalenes,[12] trietycephene,[13] cyclophane,[14] and helicene,[15] have been employed to construct intramolecular π-stacked systems. However, most of them have complicated and laborious synthetic routes with the low yields owing to the existence of the large strain forces. Examples were rare investigated in the framework of organic electronics.

Designing and synthesizing intramolecular organic π-stacked molecules are the first step to explore the unique functionalities of supramolecular organic semiconductors (SOSs) and devices. In our previous works, we found that a diarylfluorene with the unique intramolecular π–π stacking motifs in the X-ray crystallography.[16,17] In the articles, we ingeniously constructed intramolecular π-stacked molecules as SOS by designing the *ortho*-substituted steric hindrance of diarylfluorenes. A series of intramolecular π-stacked molecules had been successfully synthesized via $BF_3 \cdot Et_2O$-catalyzed Friedel–Crafts reactions (BFR). Their chemical structures and π-stacked motifs had been unambiguously confirmed by the X-ray crystallography, ^{1}H NMR, ^{13}C NMR spectra, and elemental analysis. There was an anomalous excimer electroluminescence in the organic light-emitting device with a configuration of ITO/MoO$_x$(2 nm)/NPB(30 nm)/DPBPFT(30 nm)/TPBi(10 nm)/Bebq$_2$(30 nm)/LiF(1 nm)/Al.

---

* Corresponding authors. Tel./fax: +86 25 8586 6396; e-mail addresses: iamlhxie@njupt.edu.cn (L.-H. Xie), iamwhuang@njupt.edu.cn, iamdirector@fudan.edu.cn (W. Huang).

0040-4020/$ – see front matter © 2013 Published by Elsevier Ltd.
http://dx.doi.org/10.1016/j.tet.2013.02.090

2. Results and discussion

2.1. Synthesis

Before we synthesized various intramolecular π-stacked 3diarylfluorenes with the *ortho*-substituted steric hindrance effect, we first examined the BFR of tertiary alcohols with the 3-phenylthiophene derivatives according to our previous works.[17] We found that the reaction time highly impacted on the production, as depicted in Scheme 1. The BFR of 3-phenylthiophenes occurred first in the 2-position to give *ortho*-substituted diarylfluorenes (TP-2PF) with intramolecular π-stacked motifs at a yield of 60% at reaction time of ∼2 h.

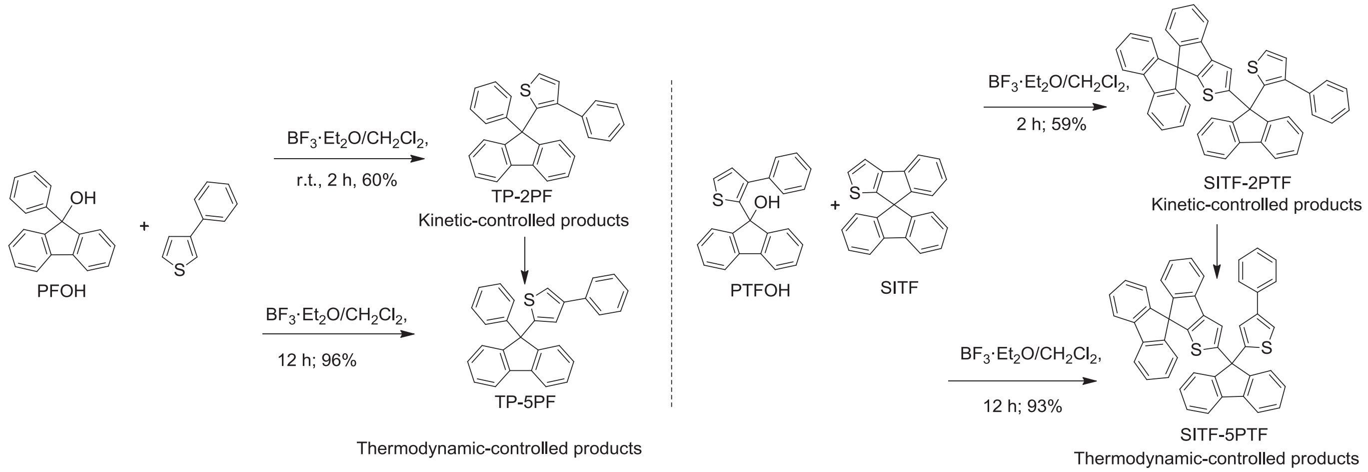

Scheme 1. Kinetic and thermodynamic-controlled processes of BF$_3$·Et$_2$O-mediated Friedel–Crafts reaction (BFR).

Interestingly, a counterpart isomer (TP-5PF) with the 5-position substitution of 3-phenylthiophenes was obtained when reaction time was extended to 12 h and the conversion yield of 96%. It was reasonable to explain that the former were kinetic-controlled products while the latter were thermodynamic-controlled products. It is expected that electrophilic substitution occurs initially at 2-postion of thiophene because the 9-phenylfluorenyl moieties are an activating group. It was known that the Friedel–Craft reactions are reversible process. The product of TP-2PF is congested molecule with higher steric hindrance and strain force than the isomer TP-5PF that favored thermodynamic reaction control. When the reaction time elongates, TP-5PF takes prevalence over less favorable TP-2PF by chemical equilibration. This similar process also has been observed in another BFR of PTFOH with SITF to give the SITF–2PTF and SITF–5PTF with the yield of 59% at the reaction time of 2 h and 93% at the reaction time of 12 h, respectively. The explain can be also supported by the electrophilic substituted bromination of 3-phenylthiophene according to the literature.[18] Furthermore, time-dependent Friedel–Crafts reactions under the catalyzed BF$_3$ and boron tris(trifluoromethanesu1fonate) were ever observed by Olah et al..[19] However, it does still not make sure the reaction mechanism suffer from the cationic process in consideration of the formation byproduct of dehydroxy 9-phenylfluorene according to our previous observation.[17]

After the above analysis, several intramolecular π-stacked diarylfluorenes were designed and synthesized by BFR of tertiary alcohols with different electron-rich arylthiophenes, as shown in Scheme 2. BFR of 3-phenylthiophene and 3,4-diphenylthiophene with PFOH of about 2 equiv at the same condition gave the products PBPFT and DPBPFT with the yields of 65% and 85%, respectively. The yield of reported DPTF (Scheme 2) was improved to 63% from 10% under HCl/AcOH.[16] Chemical structures of the above products were confirmed by ^{1}H and ^{13}C NMR, X-ray crystallography, and elements analysis. In order to confirm the intramolecular π-stacked motifs in *ortho*-substituted diarylfluorenes, X-ray crystallography and NMR spectra as well as theoretically calculation were conducted to make comparison with the corresponding isomers.

2.2. Crystal structure

Crystal structure is the most direct visible tool for π-stacked motifs. Fortunately, single crystals of TP-2PF (Fig. 1a, b) and DPBPFT (Fig. 1c, d) were obtained from a CH$_2$Cl$_2$/alcohol solution. TP-2PF and DPBPFT showed typical congested molecules with obviously intramolecular π-stacked motifs between fluoren-9-yl rings and phenyl groups at the 3-position of thiophene cores. The distance between these two kinds of face-to-face stacked groups (Fig. 1b) in TP-2PF was in the range of 3.118–4.378 Å, which was a nonparallel stacked mode owing to the steric hindrance effect. Furthermore, fluoren-9-yl rings exhibited an obvious bend curve owing to the same effect, which offered an important tool to control the curve of

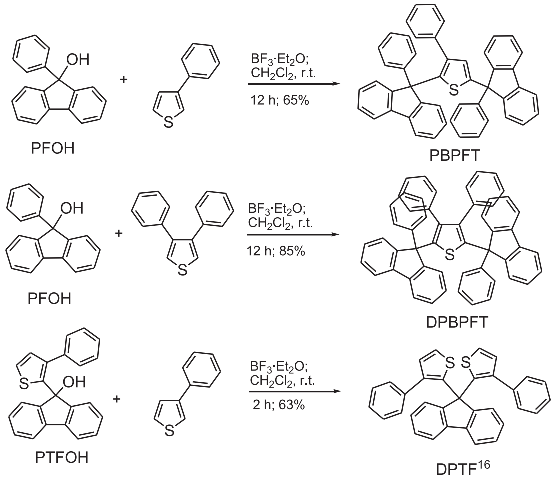

Scheme 2. The syntheses of the intramolecular π-stacked molecules via the BFR of phenylfluorenyl tertiary alcohol (PFOH) with different thiophene substrates with the *ortho*-substituted steric hindrance effect.

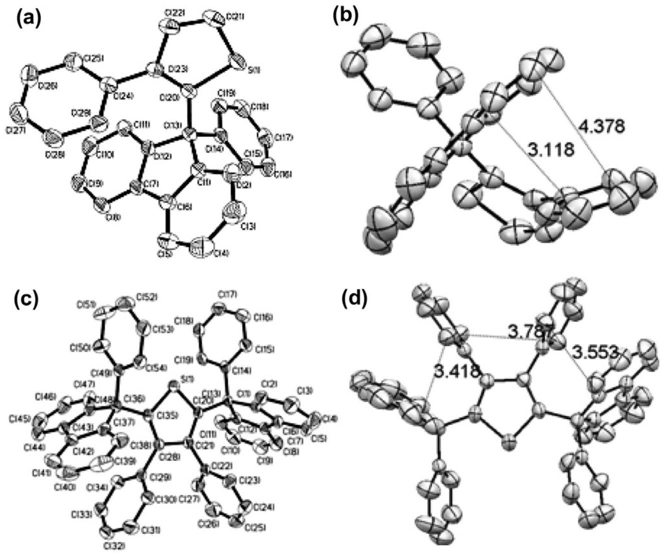

Fig. 1. Single crystal X-ray structures of TP-2PF (a, b) and DPBPFT (c, d) with ORTEP drawing and the distances of intramolecular π-stacked motifs.

aromatics with different electronic structures. DPBPFT as a strained molecules exhibited the unique gear-shaped configuration with the π-stacked distance of 3.418, 3.553, and 3.787 Å (Fig. 1d). Other modeling diarylfluorene-based intramolecular π-stacked molecules without crystal structures have been conducted to simulate the optimized molecular configurations as shown in Table S1. They also exhibited corresponding intramolecular π–π stacking interactions. It should be noted that they are antiparallel trapezium-shaped π-stacked systems. The optimized molecular geometries also had been calculated by theoretical simulation (Table S1). The distances of aryl–aryl plane were confirmed to be in the range of 3.4–3.8 Å, which offered new channel for the charge transfer and energy transfer.

2.3. ^{1}H NMR

Chemical shifts of the protons of reaction molecules are highly shielded in the NMR spectrum owing to intramolecular π-stacked interactions.[20] Fig. 2 shows the ^{1}H NMR spectra of these compounds characterized in $CDCl_3$. For TP-5PF without intramolecular π-stacked motifs, its NMR exhibits the typical aromatic chemical shift zone among 7.00–7.50 ppm at the corresponding protons of a, b, and c of thiophene–phenyls, which is reasonable according to the literature.[21] With respect to TP-5PF, the doublets and triplets of protons a, b, and c exhibit upfield shift to 6.38, 6.80, and 6.91 ppm for TP-2PF. With the increasing intensity of π–π stacking interactions, regular upfield shifts are also observed in PBPFT with the a, b, c peaks of 6.30, 6.72, and 6.84 ppm and DPBPFT with 5.84, 6.35, and 6.50 ppm, respectively. Undoubtedly, these upfield shift phenomena could be ascribed to electromagnetic shielding effect from the intramolecular rotation constrained and mutually stacking interactions between thiophene–phenyl and fluorenyl groups.

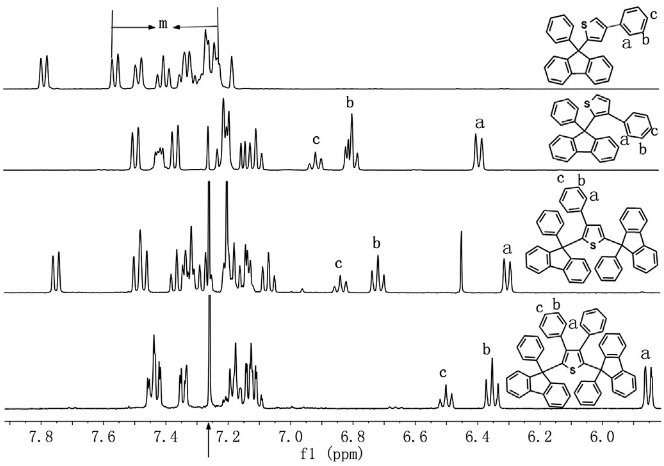

Fig. 2. The aromatic region of ^{1}H NMR (400 MHz, $CDCl_3$) spectra of TP-5PF, TP-2PF, PBPFT, and DPBPFT with part well-defined resonance assignments (signals marked by a, b, c, and m, etc. ascribe to corresponding protons; signals on vertical top of the arrow were from residual $CHCl_3$ in $CDCl_3$).

2.4. Photophysical properties

To further explore their optoelectronic properties, UV–vis absorption and photoluminescence (PL) spectra of TP-5PF, TP-2PF, PBPFT, and DPBPFT have been performed. As shown in Fig. 3a, it presents similar absorbance profiles above all, where the two distinct feature absorption bands were located at around 265 and 310 nm in their diluted solutions.[22] A sharp peak at 312 nm was

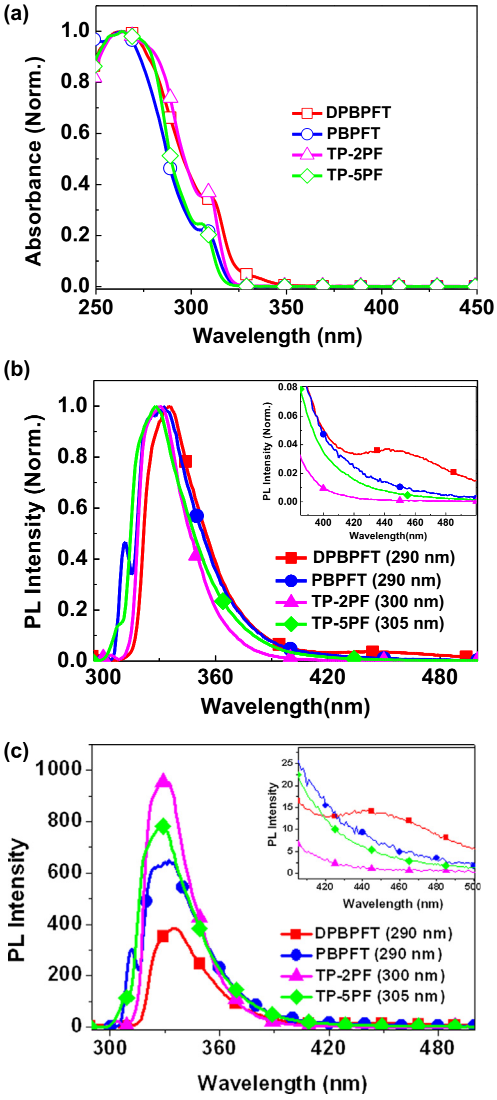

Fig. 3. The normalized UV–vis absorption (a) and PL (b) of TP-5PF, TP-2PF, PBPFT, and DPBPFT in chloroform (10^{-6} mol/L) (inset one is a magnified image of PL spectra.). (c) Their original photoluminescence in chloroform (10^{-6} mol/L) (inset one is magnified image.).

observed in DPBPFT that has 5 nm red-shift when making comparison with that of PBPFT at 307 nm. Similarly, the kinetic controlled TP-2PF offered another 4 nm red-shift in its low-energy absorption peak at 309 nm when compared with 305 nm for TP-5PF. All the UV–vis spectra exhibited concentration-dependent characteristics, which might be due to restricted motion under the high concentration, resulting in a new tailed absorption long-wavelength band (See S8b). The PL profile of PBPFT (blue dot line) has two emission bands, with a unique sharp peak at 312 nm. DPBPFT (red square line) exhibited gradually ca. 4 nm red-shift from 332 nm (PBPFT) to 336 nm as an additional phenyl substitution at 5-position of thiophene moiety. Furthermore, the thermodynamic controlled isomer TP-5PF lead to a 3 nm red-shift as 331 nm with a longer tailed band 360–400 nm, compared with TP-2PF (328 nm, triangle pink line). Noted that, a broad band between ca. 420 and 480 nm of DPBPFT was observed (inset of Fig. 3b), considered as excimer (no absorbance at longer wavelength in Fig. 3a), which provide robust evidence of the existence of the stronger intramolecular π-stacks in DPBPFT than PBPFT, TP-2PF, and TP-5PF from the normalized and original PL spectra of these compounds.

2.5. Device

Multilayer supramolecular organic light-emitting diodes (SOLEDs) were fabricated to investigate the electroluminescence of diarylfluorene-based intramolecular π-stacked molecules with the device configurations of (A): ITO/MoO_x(2 nm)/NPB(30 nm)/DPBPFT(30 nm)/TPBi(40 nm)/LiF(1 nm)/Al; and (B): ITO/MoO_x(2 nm)/NPB(30 nm)/DPBPFT(30 nm)/TPBi(10 nm)/$Bebq_2$(30 nm)/LiF(1 nm)/Al. DPBPFT (See SD). The current density–voltage and luminance–voltage characteristics for devices A and B were plotted in Fig. 4a, together with their EL spectra of DPBPFT (Fig. 4b, c). DPBPFT-based devices showed two distinctly major peaks at ca. 435 nm for A (ca. 442 nm for B) and ca. 650 nm for A (ca. 650 nm for B) under different current density. The first peaks originated from the excimer emission of the intramolecular π-stacked motifs. The second peaks were similar to that of π-stacked PVK likely due to the electromers or triplet exciton according to the literature.[6,23] These EL results indicated the existence of the intramolecular π-stacked motifs, offering a well-defined model to investigate the origin of ca. 620–680 nm under the conditions of variable-temperature and magnetic fields for supramolecular spintronics. DPBPFT-based device B displayed blue color with Commission Internationale de l'Eclairage (CIE) coordinates of (0.21, 0.16) under the voltage of 15 V. Compared with device A, device B exhibited a maximum luminance of ca. 1282 cd/m^2 with a luminous efficiency of 0.24 cd/A and a turn-on voltage of 9 V.

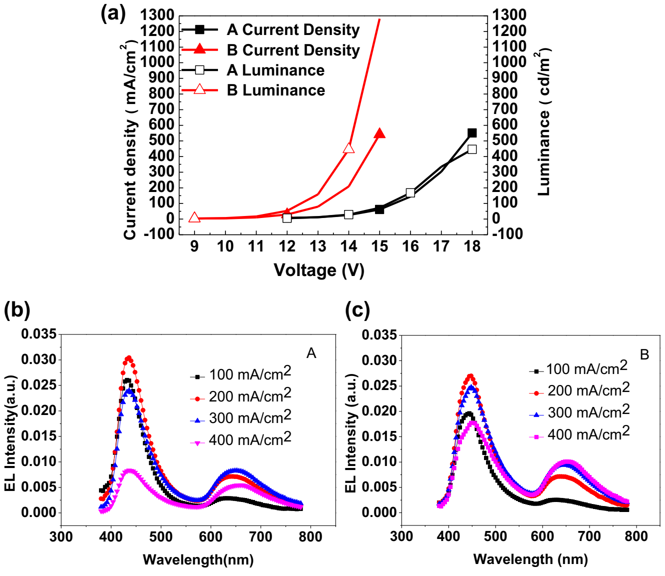

Fig. 4. Current density–voltage–luminance (a) and EL spectra of the OLED devices A (b) and B (c) made by DPBPFT.

3. Conclusion

We have observed thermodynamic-controlled and kinetic-controlled processes in the $BF_3 \cdot Et_2O$-catalyzed Friedel–Crafts reaction (BFR) of tertiary alcohols. A series of complex diarylfluorenes-based intramolecular π-stacked molecules as the SOS models have been synthesized by means of the *ortho*-substituted steric hindrance design via the key step of the BFR at the yields of 60–85%. Intramolecular π-stacked motifs in these organic complexes result in an excimer emission in the concentrated solution. Supramolecular light-emitting devices (SLEDs) have been fabricated with unique electroluminescent spectra, brightness of 1282 cd/m^2 and current efficiency of 0.24 cd/A. Organic complexes and supramolecular devices offer the unique models to investigate structure–function relationship for organic electronics, optoelectronics, mechatronics, and spintronics.

4. Experimental section

4.1. General information

4.1.1. Chemicals. Magnesium turnings, thiophene, and fluorenone were used without further purification. 3-Phenylthiophene, 2,5-dibromo-3-phenylthiophene, 3,4-diphenylthiophene, 9-phenyl-fluoren-9-ol,[24] and 9-(3-phenylthiophen-2-yl)-fluoren-9-ol, were prepared as previously reported.[16] THF and diethyl ether were dried over sodium benzophenone ketyl anion radical and distilled under a dry nitrogen atmosphere immediately prior to use. All reactions involving organometallic reagents were carried out under nitrogen.

4.1.2. Characterization. ^1H and ^{13}C NMR in $CDCl_3$ was recorded at 400 MHz. Chemical shifts were reported in parts per million (δ), and the signals were designated as follows: s (singlet), d (doublet), t (triplet), and m (multiplet). For the MALDI–TOF MS spectra, the spectra were recorded in reflective mode, and no substrate was used. Absorption spectra (1 μM in $CHCl_3$) were measured at 25 °C, and emission spectra (1 μM in $CHCl_3$) were recorded upon excitation at the absorption maxima in the degassed $CHCl_3$ solvent after saturating with argon. Differential scanning calorimetry (DSC) analyses were performed under N_2, the samples were ramped at 10 °C/min from 30 °C to 360 °C, then quenched at 10 °C/min to room temperature. Thermogravimetric analyses (TGA) were performed conducted under a heating rate of 10 °C/min and a nitrogen flowing rate of 20 cm^3/min. Geometry optimizations and electronic analysis were carried out at the B97-D[25,26] including R^{-6} project and TZVP[27,28] basis sets with polarization functions (except for hydrogen).

4.2. Data for X-ray structure analysis

Crystallographic data for TP-2PF and DPBPFT were saved as the files of CCDC 817167.cif and CCDC 817168.cif, respectively. Data were collected at room temperature on a detector with graphite-monochromated Mo Kα radiation (λ=0.71073 Å). The absorption correction was applied by integration based on the crystal shape. Structures were solved by direct methods and refined against F^2 with the full-matrix and least-squares methods. Hydrogen atoms were found by difference Fourier syntheses and were refined.

4.2.1. *Crystal data for TP-2PF.* $C_{29}H_{20}S$, M=400.53, T=273(2) K, monoclinic, $C2/c$, Z=8, a=27.159(4) Å, b=7.6566(12) Å, c=20.530(3) Å, α=90°, β=100.852(3)°, γ=90°, V=4192.9(12) Å^{3}, F(000)=1680, ρ_{calcd}=1.269 Mg m^{-3}, μ (Mo Kα)=0.168 mm^{-1}, $2\theta_{max}$=52°, reflections collected/unique 10,633/4091 (R_{int}=0.0564), parameters 271, Final $R1$=0.0402 ($I>2\sigma(I)$), $wR2$=0.1075 ($I>2\sigma(I)$), $R1$=0.0564 (all data), $wR2$=0.1125 (all data), S=0.948 (all data).

4.2.2. *Crystal data for DPBPFT.* $C_{54}H_{36}S$, M=716.93, T=291(2) K, monoclinic, $P21/c$, Z=4, a=12.007(10) Å, b=13.674(11) Å, c=26.541(17) Å, α=90.00°, β=116.90(3)°, γ=90.00°, V=3886(5) Å^{3}, F(000)=1504, ρ_{calcd}=1.225 Mg m^{-3}, μ (Mo Kα)=0.121 mm^{-1}, $2\theta_{max}$=49.98°, reflections collected/unique 18,874/6856 (R_{int}=0.1182), parameters 496, Final $R1$=0.0569 ($I>2\sigma(I)$), $wR2$=0.0979 ($I>2\sigma(I)$), $R1$=0.1430 (all data), $wR2$=0.1219 (all data), S=0.827 (all data). Crystal data for CCDC 817167 and 817168 contained the supplementary crystallographic data for this paper. These data can be obtained free of charge from The Cambridge Crystallographic Data Centre via www.ccdc.cam.ac.uk/data_request/cif.

4.3. Device fabrication and characterization

All the devices were fabricated onto pre-patterned indium–tin oxide (ITO) with a sheet resistance of 10 Ω/sq. The substrates were sonicated sequentially with detergent, 2-propanol, acetone, and deionized water, then dried in an oven, and finally treated in an ultraviolet–ozone chamber. After the organic deposition, 100 nm-thick Al was covered directly on the organic layers to serve as cathode. The cathode area defines an active device area of 2×2 mm^{2} through a shadow mask. EQE was measured in an integrated sphere, following the method mentioned in the literature.[8,10,29] All measurements were carried out in ambient environment without encapsulation. Two potential undoped devices (A, B) of DPBPFT were fabricated with multilayer configurations. Configuration of device A ITO/MoO_x(2 nm)/NPB(30 nm)/DPBPFT (30 nm)/TPBi(40 nm)/LiF (1 nm)/Al; $Bebq_2$ was added in device B. Configuration of device B ITO/MoO_x(2 nm)/NPB(30 nm)/DPBPFT(30 nm)/TPBi(10 nm)/$Bebq_2$(30 nm)/LiF(1 nm)/Al. All devices had the same total thickness of organic films (100 nm). In devices A and B, DPBPFT served as the blue light emitter, a thin-layer MoO_x (2 nm) and LiF (1 nm) acted as anode and cathode buffer layers, and NPB acted as the hole-injecting and transporting layers. $Bebq_2$ and TPBi were used as the electron-transporting layer and hole/exciton blocking layer. NPB represents *N*,*N*′-diphenyl-*N*,*N*′-bis(1,1′-biphenyl)-4,4′-diamine, TPBi represents 1,3,5-tris-(*N*-phenylbenzi-midazole-2-yl)-benzene, and $Bebq_2$ represents bis(10-hydroxybenzo[*h*]qinolinato) beryllium. Fig. 4 compares the luminance (*L*)–voltage (*V*)–current density (*J*) characteristics, CE–luminance–power efficiency (PE) characteristics, normalized EL spectra, and external quantum efficiencies of devices A and B, respectively.

4.4. General procedure for Friedel–Crafts reaction of 9-phenyl-fluoren-9-ol (PFOH) and 9-(3-phenylthiophen-2-yl)-fluoren-9-ol (PTFOH) with various aryl substrates

A solution of $BF_3\cdot Et_2O$ in appropriate dichloromethane (15 mL) was added dropwise to the mixed solution of tertiary alcohols and aryl substrates in dichloromethane of appropriate amount (60 mL). The reaction mixture was stirred at room temperature (25 °C) until starting material was no longer detectable by TLC (2–12 h). Ethanol (10 mL) and water (30 mL) were successively added to quench the reaction. Different phases were then separated and the aqueous phase was extracted with dichloromethane. The combined dichloromethane layers were washed and dried with anhydrous $MgSO_4$. After removal of the solvent, the remaining crude product was purified by silicon gel chromatography (petroleum ether–dichloromethane) to yield the final products.

4.4.1. *3-Phenyl-2-(9-phenyl-fluoren-9-yl)thiophene (TP-2PF).* This compound was prepared following the above-mentioned general procedures using 3-phenylthiophene (1.60 g, 10 mmol, 1 equiv), 9-phenyl-fluoren-9-ol (2.84 g, 11 mmol, 1.1 equiv), and $BF_3\cdot Et_2O$ (1.5 mL, 12 mmol, 1.2 equiv). After 2 h of reaction, 2.40 g TP-2PF was obtained with a 60% yield. Mp: 127 °C. GC/MS (*m*/*z*): 400 (M^{+}). ^{1}H NMR (400 MHz, $CDCl_3$, ppm) δ: 6.38–6.40 (d, J=7.7, 2H), 6.78–6.82 (m, 3H), 6.90–6.93 (t, J=7.2, 1H), 7.09–7.12 (t, J=7.5, 2H), 7.14–7.15 (d, J=5.2, 1H), 7.19–7.21 (m, 4H), 7.23 (s, 1H), 7.35–7.37 (d, J=7.7, 2H), 7.40–7.43 (m, 2H), 7.48–7.50 (d, J=7.5, 2H). ^{13}C NMR (100 MHz, $CDCl_3$, ppm) δ: 150.2, 145.9, 143.4, 140.28, 140.0, 137.1, 131.6, 128.9, 128.0, 127.9, 127.5, 127.2, 126.9, 126.6, 125.9, 122.1, 119.9, 61.9. Anal. Calcd for: $C_{29}H_{20}S$: C, 86.96; H, 5.03; Found: C, 86.99; H, 5.22.

4.4.2. *3-Phenyl-5-(9-phenylfluoren-9-yl)thiophene (TP-5PF).* This compound was prepared following the reacting condition above using TP-2PF (0.40 g, 1.0 mmol, 1 equiv) and $BF_3\cdot Et_2O$ (0.15 mL, 1.2 mmol, 1.2 equiv). After 12 h of reaction, 0.38 g TP-5PF was obtained with the yield of 96%. GC/MS (*m*/*z*): 400 (M^{+}). Mp: 146 °C. ^{1}H NMR (400 MHz, $CDCl_3$, ppm) δ: 7.18 (s, 1H), 7.21–7.24 (m, 3H), 7.27–7.30 (m, 4H), 7.32–7.35 (m, 4H) 7.38–7.42 (t, J=7.4, 2H), 7.47–7.49 (d, J=7.9, 2H), 7.55–7.57 (d, J=7.6, 2H), 7.78–7.79 (d, J=7.5, 2H). ^{13}C NMR (100 MHz, $CDCl_3$, ppm) δ: 150.9, 150.3, 145.2, 141.5, 139.9, 135.9, 128.7, 128.3, 128.0, 127.8, 127.7, 127.1, 127.1, 126.3, 126.2, 125.7, 120.3, 119.3, 62.4. Anal. Calcd for: $C_{29}H_{20}S$: C, 86.96; H, 5.03; Found: C, 86.80; H, 5.18.

4.4.3. *3-Phenyl-2,5-bis(9-phenylfluoren-9-yl)thiophene (PBPFT).* This compound was synthesized according to the general procedures above using 3-phenylthiophene (0.322 g, 2 mmol, 1 equiv), 9-phenyl-fluoren-9-ol (1.14 g, 4.4 mmol, 2.2 equiv), and $BF_3\cdot Et_2O$ (0.6 mL, 4.8 mmol, 2.4 equiv). After 12 h of reaction, starting material was no longer detectable by TLC, the yield of PBPFT was 65%. Mp: 145 °C. ^{1}H NMR (400 MHz, $CDCl_3$, ppm) δ: 6.29–6.31 (d, J=7.7, 2H), 6.45 (s, 1H), 6.70–6.74 (t, J=7.6, 2H), 6.82–6.86 (t, J=7.4, 1H), 7.05–7.09 (t, J=7.5, 2H), 7.13–7.14 (m, 3H), 7.16 (s, 1H), 7.18 (s, 1H), 7.20–7.21 (m, 5H), 7.27–7.29 (d, J=7.5, 2H), 7.31–7.33 (m, 4H), 7.33–7.38 (t, J=7.5, 2H) 7.46–7.50 (t, J=8.3, 4H), 7.74–7.76 (d, J=7.5, 2H). ^{13}C NMR (100 MHz, $CDCl_3$, ppm) δ: 150.7, 150.1, 146.1, 145.6, 144.9, 142.5, 139.9, 139.8, 138.9, 137.1, 130.8, 128.8, 128.1, 127.9, 127.8, 127.7, 127.5, 127.4, 127.2, 127.1, 126.9, 126.7, 126.6, 126.3, 125.7, 120.2, 119.8, 62.2, 62.1. Anal. Calcd for: $C_{48}H_{32}S$: C, 89.96; H, 5.03; Found: C, 89.90; H, 5.14.

4.4.4. *3,4-Diphenyl-2,5-bis(9-phenylfluoren-9-yl)thiophene (DPBPFT).* This compound was prepared following the general procedures above using 3,4-diphenylthiophene (0.236 g, 1.0 mmol 1 equiv), 9-phenyl-fluoren-9-ol (0.57 g, 2.2 mmol, 2.2 equiv), and $BF_3\cdot Et_2O$ (0.30 mL, 2.4 mmol, 2.4 equiv). After 12 h of reaction, 0.61 g DPBPFT was obtained with 85% yield. ^{1}H NMR (400 MHz, $CDCl_3$, ppm) δ: 5.84–5.86 (d, J=7.0, 4H), 6.33–6.37 (t, 4H), 6.48–6.52 (t, 2H), 7.09–7.11 (d, J=1.5, 2H), 7.12–7.13 (t, J=1.7, 4H), 7.14–7.144 (d, J=1.3, 2H), 7.16–7.19 (m, 6H), 7.33 (s, 2H), 7.35–7.36 (d, J=1.8, 2H) 7.418–7.422 (d, J=1.7, 2H), 7.44 (s, 4H), 7.45–7.46 (d, J=2.0, 2H). ^{13}C NMR (100 MHz, $CDCl_3$, ppm) δ: 150.5, 145.7, 141.7, 140.5, 140.0, 135.9, 130.1, 128.0, 127.8, 127.1, 127.1, 127.1, 126.5, 125.8, 125.0, 119.8, 62.1. Anal. Calcd for: $C_{54}H_{36}S$: C, 90.47; H, 5.06; Found: C, 90.41; H, 5.12.

4.4.5. *2′-(9-(4-Phenylthiophen-2-yl)-fluoren-9-yl)spiro[fluorene-9,8′-indeno[2,1-b]thiophene] (SITF–5PTF).* This compound was synthesized according to the reacting condition as TP-2PF using

2′-(9-(3-phenylthiophen-2-yl)-fluoren-9-yl)spiro[fluorene-9,8′-indeno[2,1-*b*]thiophene] (SITF–2PTF) (0.645 g, 1.0 mmol, 1 equiv) and $BF_3 \cdot Et_2O$ (0.15 mL, 1.2 mmol, 1.2 equiv). After 12 h of reaction, starting material was no longer detectable by TLC, 0.60 g SITF–5PTF was obtained with a 93% yield. Mp: 308 °C. ^1H NMR (400 MHz, $CDCl_3$, ppm) δ: 6.55–6.57 (d, *J*=7.6, 1H), 6.80–6.82 (d, *J*=7.5, 2H), 6.90–6.94 (t, *J*=7.8, 1H), 7.09–7.13 (t, 2H), 7.21–7.22 (m, 2H), 7.23–7.25 (m, 2H), 7.31–7.35 (m, 7H), 7.39–7.43 (t, 2H), 7.45–7.46 (m, 3H), 7.70–7.72 (d, *J*=7.6, 2H), 7.74–7.76 (d, *J*=7.5, 4H) ^{13}C NMR (100 MHz, $CDCl_3$, ppm) δ: 154.0, 152.3, 150.1, 149.8, 148.2, 147.5, 146.5, 141.5, 141.4, 139.4, 139.1, 135.8, 128.7, 128.4, 128.0, 127.8, 127.8, 127.4, 127.1, 126.3, 126.0, 125.4, 125.4, 123.9, 123.3, 120.3, 120.0, 119.5, 119.2, 117.8, 64.3, 59.9. Anal. Calcd for: $C_{46}H_{28}S_2$: C, 85.68; H, 4.38; Found: C, 85.70; H, 4.35.

Acknowledgements

The authors acknowledge financial support from National Basic Research Program of China (973 Program, 2009CB930601), National Natural Science Foundation of China (21274064, BZ2010043, 20974046, 20774043, 51173081, 50428303, 61136003, 21144004, 51273092, 61106058), the Program for New Century Excellent Talents in University (NCET-11-0992), Natural Science Foundation of Jiangsu Province (BK2011761, BK2008053, BK2009025, 10KJB510013).

Supplementary data

Copies of ^1H NMR and ^{13}C NMR for all new compounds, as well as X-ray and TGA data for TP-2PF and DPBPFT; PL spectra, DSC, and normalized EL (for DPBPFT) data, as well as geometry optimized structures for all new compounds. Supplementary data related to this article can be found at http://dx.doi.org/10.1016/j.tet.2013.02.090.

References and notes

1. Lehn, J. M. *Supramolecular Chemistry: Concepts and Perspectives*; VCH: Weinheim, 1995.
2. (a) Meyer, E. A.; Castellano, R. K.; Diederich, F. *Angew. Chem., Int. Ed.* **2003**, *42*, 1210; (b) Bhosale, S.; Sisson, A. L.; Talukdar, P.; Fürstenberg, A.; Banerji, N.; Vauthey, E.; Bollot, G.; Mareda, J.; Röger, C.; Würthner, F.; Sakai, N.; Matile, S. *Science* **2006**, *313*, 84.
3. Burattini, S.; Colquhoun, H. M.; Greenland, B. W.; Hayes, W.; Wade, M. *Macromol. Rapid Commun.* **2009**, *30*, 459.
4. (a) Hardouin-Lerouge, M.; Hudhomme, P.; Salle, M. *Chem. Soc. Rev.* **2011**, *40*, 30; (b) Legouin, B.; Uriac, P.; Tomasi, S.; Toupet, L.; Bondon, A.; Weghe, P. V. D. *Org. Lett.* **2009**, *11*, 745; (c) Nguyen, J. Q.; Iverson, B. L. *J. Am. Chem. Soc.* **1999**, *121*, 2639; (d) Kelly, T. R. *Acc. Chem. Res.* **2001**, *34*, 514.
5. Watson, J. D.; Crick, F. H. C. *Nature* **1953**, *171*, 737.
6. (a) *Nat. Mater* **2008**, *7*, 267; (b) Xie, L. H.; Ling, Q. D.; Hou, X. Y.; Huang, W. *J. Am. Chem. Soc.* **2008**, *130*, 2120; (c) Xie, L. H.; Deng, X. Y.; Chen, L.; Chen, S. F.; Liu, R. R.; Hou, X. Y.; Wong, K. Y.; Ling, Q. D.; Huang, W. *J. Polym. Sci., Part A: Polym. Chem.* **2009**, *47*, 5221.
7. Nandy, R.; Subramoni, M.; Varghese, B.; Sankararaman, S. *J. Org. Chem.* **2007**, *72*, 938.
8. Yoo, H.; Yang, J.; Yousef, A.; Wasielewski, M.; Kim, D. *J. Am. Chem. Soc.* **2010**, *132*, 3939.
9. (a) Vura-Weis, J.; Abdelwahed, S. H.; Shukla, R.; Rathore, R.; Ratner, M. A.; Wasielewski, M. R. *Science* **2010**, *328*, 1547; (b) Thirion, D.; Poriel, C.; Barriere, F.; Metivier, R.; Jeannin, O.; Rault-Berthelot, J. *Org. Lett.* **2009**, *11*, 4794; (c) Nakano, T.; Yade, T. *J. Am. Chem. Soc.* **2003**, *125*, 15474; (d) Nakano, T.; Takewaki, K.; Yade, T.; Okamoto, Y. *J. Am. Chem. Soc.* **2001**, *123*, 9182.
10. (a) Casarini, D.; Rosini, C.; Grilli, S.; Lunazzi, L.; Mazzanti, A. *J. Org. Chem.* **2003**, *68*, 1815; (b) Casarini, D.; Grilli, S.; Lunazzi, L.; Mazzanti, A. *J. Org. Chem.* **2004**, *69*, 345; (c) Lunazzi, L.; Mazzanti, A.; Rafi, S.; Rao, H. S. P. *J. Org. Chem.* **2008**, *73*, 678.
11. (a) Lunazzi, L.; Mancinelli, M.; Mazzanti, A. *J. Org. Chem.* **2008**, *73*, 2198; (b) Lunazzi, L.; Mancinelli, M.; Mazzanti, A. *J. Org. Chem.* **2007**, *72*, 10045; (c) Casarini, D.; Lunazzi, L.; Mazzanti, A. *Eur. J. Org. Chem.* **2010**, *2010*, 2035.
12. (a) Zoltewicz, J. A.; Maier, N. M.; Fabian, W. M. F. *J. Org. Chem.* **1996**, *61*, 7018; (b) Morisaki, Y.; Fernandes, J. A.; Chujo, Y. *Polym. J.* **2010**, *42*, 928.
13. (a) Gung, B. W.; Patel, M.; Xue, X. *J. Org. Chem.* **2005**, *70*, 10532; (b) Gung, B. W.; Wekesa, F.; Barnes, C. L. *J. Org. Chem.* **2008**, *73*, 1803; (c) Gung, B. W.; Xue, X.; Reich, H. J. *J. Org. Chem.* **2005**, *70*, 3641.
14. (a) Watson, M. D.; Jäckel, F.; Severin, N.; Rabe, J. P.; Müllen, K. *J. Am. Chem. Soc.* **2004**, *126*, 1402; (b) Ramaiah, D.; Neelakandan, P. P.; Nair, A. K.; Avirah, R. R. *Chem. Soc. Rev.* **2010**, *39*, 4158.
15. (a) Takenaka, N.; Sarangthem, R. S.; Captain, B. *Angew. Chem., Int. Ed.* **2008**, *47*, 9708; (b) Miyasaka, M.; Pink, M.; Rajca, S.; Rajca, A. *Angew. Chem., Int. Ed.* **2009**, *48*, 5954.
16. Xie, L. H.; Fu, T.; Hou, X. Y.; Tang, C.; Hua, Y. R.; Wang, R. J.; Fan, Q. L.; Peng, B.; Wei, W.; Huang, W. *Tetrahedron Lett.* **2006**, *47*, 6421.
17. Xie, L. H.; Hou, X. Y.; Hua, Y. R.; Tang, C.; Liu, F.; Fan, Q. L.; Huang, W. *Org. Lett.* **2006**, *8*, 3701.
18. Gronowitz, S.; Gjos, N.; Kellogg, R. M.; Wynberg, H. *J. Org. Chem.* **1967**, *32*, 463.
19. (a) Olah, G. A.; Olah, J. A.; Ohyama, T. *J. Am. Chem. Soc.* **1984**, *106*, 5284; (b) Olah, G. A.; Farooq, O.; Farnia, S. M. F.; Olah, J. A. *J. Am. Chem. Soc.* **1988**, *110*, 2560.
20. Chen, S. S.; Yan, Q. F.; Li, T.; Zhao, D. H. *Org. Lett.* **2010**, *12*, 4784.
21. Pei, J.; Ni, J.; Zhou, X. H.; Cao, X. Y.; Lai, Y. H. *J. Org. Chem.* **2002**, *67*, 4924.
22. Hou, X. Y.; Li, T. C.; Yin, C. R.; Xu, H.; Lin, J.; Hua, Y. R.; Chen, D. Y.; Xie, L. H.; Huang, W. *Synth. Met.* **2009**, *159*, 1055.
23. (a) Qian, L.; Bera, D.; Holloway, P. H. *Appl. Phys. Lett.* **2007**, *90*, 103511; (b) Ye, T. L.; Chen, J. S.; Ma, D. G. *Phys. Chem. Chem. Phys.* **2010**, *12*, 15410.
24. Wong, K. T.; Wang, Z. J.; Chien, Y. Y.; Wang, C. L. *Org. Lett.* **2001**, *3*, 2285.
25. Grimme, S. *J. Comput. Chem.* **2006**, *27*, 1787.
26. Grimme, S. *Angew. Chem., Int. Ed.* **2008**, *47*, 3430.
27. SchTfer, A.; Huber, C.; Ahlrichs, R. *J. Chem. Phys.* **1994**, *100*, 5829.
28. Grimme, S.; Mück-Lichtenfeld, C.; Antony, J. *J. Phys. Chem. C* **2007**, *111*, 11199.
29. (a) Meerheim, R.; Nitsche, R.; Leo, K. *Appl. Phys. Lett.* **2008**, *93*, 043310; (b) Gu, J. F.; Xie, G. H.; Zhang, L.; Chen, S. F.; Lin, Z. Q.; Zhang, Z. S.; Zhao, J. F.; Xie, L. H.; Tang, C.; Zhao, Y.; Liu, S. Y.; Huang, W. *J. Phys. Chem. Lett.* **2010**, *1*, 2849.